Konya Mühendislik Bilimleri Dergisi, c. 13, s. 3, 947-964, 2025
Konya Journal of Engineering Sciences, v. 13, n. 3, 947-964, 2025
ISSN: 2667-8055 (Electronic)
DOI: 10.36306/konjes.1676034

DRY SLIDING WEAR RESISTANCE OF AGED WOVEN CARBON AND GLASS FIBER-REINFORCED EPOXY MATRIX COMPOSITES IN DIFFERENT DEGRADATION ENVIRONMENTS

[1,*] **Ahmet SAYLIK**, [2] **Şemsettin TEMİZ**

[1] *Muş Alparslan University, Engineering and Architecture Faculty, Mechanical Engineering Department, Muş, TÜRKİYE*
[2] *Inonu University, Engineering Faculty, Mechanical Engineering Department, Malatya, TÜRKİYE*
[1]a.saylik@alparslan.edu.tr, [2]semsettin.temiz@inonu.edu.tr

Highlights

- GFRP and CFRP composites were aged in seawater, engine oil, and diesel fuel.
- Tribological performance was evaluated using dry sliding pin-on-disc tests.
- CFRP showed better aging resistance; GFRP was more sensitive to degradation.
- Aging time and environment had a significant impact on wear and friction.
- Specific wear rate and COF were influenced by load, aging, and material type.

Graphical Abstract

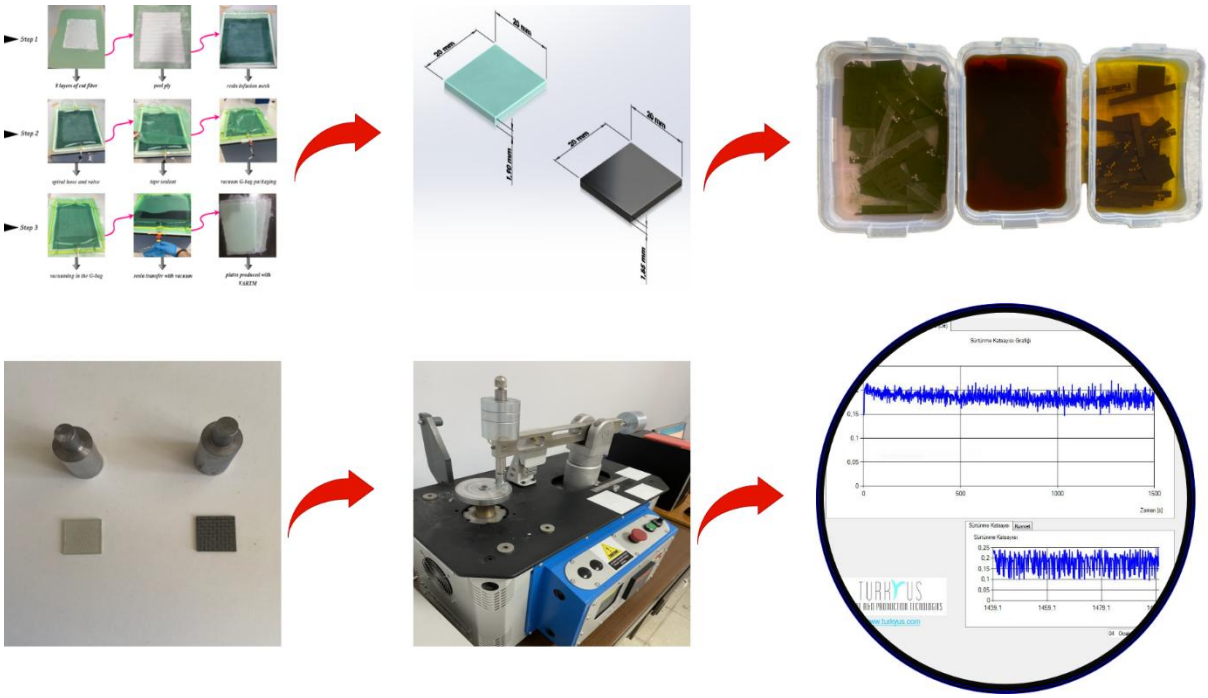

Flowchart of the proposed method

***Corresponding Author:** Ahmet SAYLIK, a.saylik@alparslan.edu.tr

Konya Mühendislik Bilimleri Dergisi, c. 13, s. 3, 947-964, 2025
Konya Journal of Engineering Sciences, v. 13, n. 3, 947-964, 2025
ISSN: 2667-8055 (Electronic)
DOI: 10.36306/konjes.1676034

DRY SLIDING WEAR RESISTANCE OF AGED WOVEN CARBON AND GLASS FIBER-REINFORCED EPOXY MATRIX COMPOSITES IN DIFFERENT DEGRADATION ENVIRONMENTS

[1,*] **Ahmet SAYLIK**, [2] **Şemsettin TEMİZ**

[1] *Muş Alparslan University, Engineering and Architecture Faculty, Mechanical Engineering Department, Muş, TÜRKİYE*
[2] *Inonu University, Engineering Faculty, Mechanical Engineering Department, Malatya, TÜRKİYE*
[1]a.saylik@alparslan.edu.tr, [2]semsettin.temiz@inonu.edu.tr

(Received: 14.04.2025; Accepted in Revised Form: 02.07.2025)

ABSTRACT: In this study, the dry sliding behavior of carbon/epoxy (CFRP) and glass/epoxy (GFRP) composites, aged for 30, 60, and 90 days in artificial seawater, engine oil, and diesel fuel environments, was experimentally tested and compared using the pin-on-disc method. The composites were manufactured using a vacuum-assisted resin transfer molding (VARTM) process, reinforced with RIM 135 epoxy polymer matrix, twill-woven glass fibers, and plain-woven carbon fibers. Wear tests were conducted following the ASTM G99-17 standard. AISI 52100 bearing steel, hardened to 65 HRC, was used as the abrasive disc, and the experiments were performed on a pin-on-disc wear testing device. The dry sliding behavior of the aged composites was examined under 10 N, 20 N, and 30 N loads using the pin-on-disc method. The results indicated that the lowest weight loss occurred in the diesel fuel environment, while the highest weight loss was observed in the engine oil environment. Furthermore, the seawater environment was found to have the least impact on the specific wear rate.

Keywords: *Degradation, Fiber Reinforced Polymer Composites, Wear, Friction, Pin on Disc, Seawater Aging*

1. INTRODUCTION

Wear is defined as the undesirable loss of material that occurs on the surfaces of bodies in contact and in relative motion due to frictional forces. Materials of machine elements exposed to wear degrade over time and can no longer perform their functions effectively. The need to combat wear has led to the development of newer materials, especially polymer-based composite materials. Fiber-reinforced polymer matrix composites are among the fastest-growing material classes in current material design and modeling, as they offer a good combination of lightness, corrosion resistance, and high specific strength [1], [2]. The most commonly used fiber types in the production of such composites are glass and carbon fibers. Laminated composites are increasingly used in the defense industry due to their superior strength, lightness, and durability. These materials are expected to resist various abrasive factors encountered in nature during military operations, such as soil, gravel, debris, and other environmental effects. The wear resistance of composites depends on factors such as the type of reinforcing fibers, the resin matrix, and surface treatments applied to enhance durability. For fiber-reinforced polymer matrix composites, wear mechanisms under dry sliding conditions include matrix wear, fiber pull-out, fiber breakage, and interfacial debonding. In literature, a low coefficient of friction is generally associated with high wear resistance. Friction and wear problems occur in almost every surface interaction involving contact. Adhesive wear typically characterizes the interaction between polymer-based materials and metal surfaces in relative motion [3]. The dry sliding test is one of the tribological methods used to evaluate the friction and wear behavior between two surfaces. The coefficient of friction is defined as the ratio of the friction force to the applied load, indicating how easily one material slides over another [4]. To enhance the wear resistance of polymer matrix composites sliding on metal surfaces under dry conditions, various fibers or polymer matrices are used. One of the most common approaches to improving the wear resistance of polymer matrices is to incorporate different types and ratios of

***Corresponding Author:** Ahmet SAYLIK, a.saylik@alparslan.edu.tr

nanoparticles uniformly within the polymer matrix [5]–[11]. Nanoparticle-reinforced polymer composites, particularly α-Al2O3 and SiO2 filled PTFE, demonstrate good wear resistance under loads ranging from 1 MPa to 10 MPa. Among them, α-Al2O3/PTFE shows superior performance due to the formation of thicker and more cohesive tribofilms [12]. Studies have been conducted to improve the tribological performance of composites exposed to deep-sea environments by reinforcing POM plastic with carbon fiber and Al2O3 nanoparticles. It was concluded that the addition of Al2O3 nanoparticles simultaneously enhanced the mechanical strength, thermal stability, and seawater resistance of the composite, with optimum properties achieved at a 4% loading of Al2O3 nanoparticles [13]. Glass, carbon, basalt, and kevlar fiber-reinforced polymer composites are commonly used in marine applications. Examples include the hulls, elbows, and sonar domes of boats and ships [14]–[17]. The mechanical and tribological performance varies depending on the fiber type, matrix type, and stacking configuration of the fiber/matrix composite structure. Glass and carbon fibers have different mechanical strengths, and their wear resistance also differs when exposed to corrosive environments. Composites subjected to corrosive media such as seawater may experience swelling, weakening, or microstructural damage due to chemical and physical degradation of the matrix. For example, with every 100 m increase in ocean depth, seawater pressure increases linearly by approximately 1 MPa, which typically leads to accelerated seawater absorption. The effects of deep-sea pressure and seawater diffusion on the tribological and mechanical performance of polymer composites remain uncertain [18]. Studies on improving the mechanical and tribological behavior of polymer matrix composites under various environmental conditions continue to be relevant [19]–[26]. The wear behavior of glass fiber-reinforced polyester (GFRP) composites under different environmental conditions was investigated. Wear tests were performed under 60 N load, 500 rpm speed, and 2-hour duration, simulating various artificial aging conditions such as acidic environments, hydrothermal cycling, and UV radiation. It was observed that the glass fiber content, varying between 11–18 wt%, significantly affected wear resistance and the coefficient of friction. Excessive glass fiber content increased the accumulation of wear debris, which led to a higher coefficient of friction [27]. The wear behavior of glass fiber-reinforced epoxy (GFRE) composites under varying environmental temperatures and thermal aging conditions was also examined. The coefficient of friction (COF) was found to be most significantly influenced by thermal aging ($p = 0.001$). The effect of sliding distance was reported as $p = 0.028$, while load changes showed no statistically significant impact on COF ($p = 0.165$) [28].

In this study, the tribological resistance of glass and carbon fiber-reinforced epoxy matrix composites aged in different liquid-based corrosive environments under dry sliding conditions was evaluated. Seawater, motor oil, and diesel fuel were used as corrosive media. The aim was to address the research gap in the literature by comparing the tribological performance of glass and carbon epoxy composites subjected to these three degradation environments. The schematic representation of the experimental procedures is presented in Figure 1.

2. MATERIAL AND METHODS

2.1. Production of Composite Materials

In the experimental study, two types of fiber reinforcements were used in the laminated composite structures: glass fiber and carbon fiber. As reinforcing elements, a 300 g/m² area density E-glass twill weave fabric and a 200 g/m² area density carbon plain weave fabric were employed. The E-glass (twill) 2x2 fiber weave refers to a pattern in which each weft and warp yarn passes over two yarns and under two yarns alternately. A single layer of E-glass fiber has an approximate thickness of 0.23 mm. The carbon (plain) fiber forms a grid-like pattern, with weft and warp yarns passing over and under each other alternately. A single layer of carbon fiber has an approximate thickness of 0.2 mm.

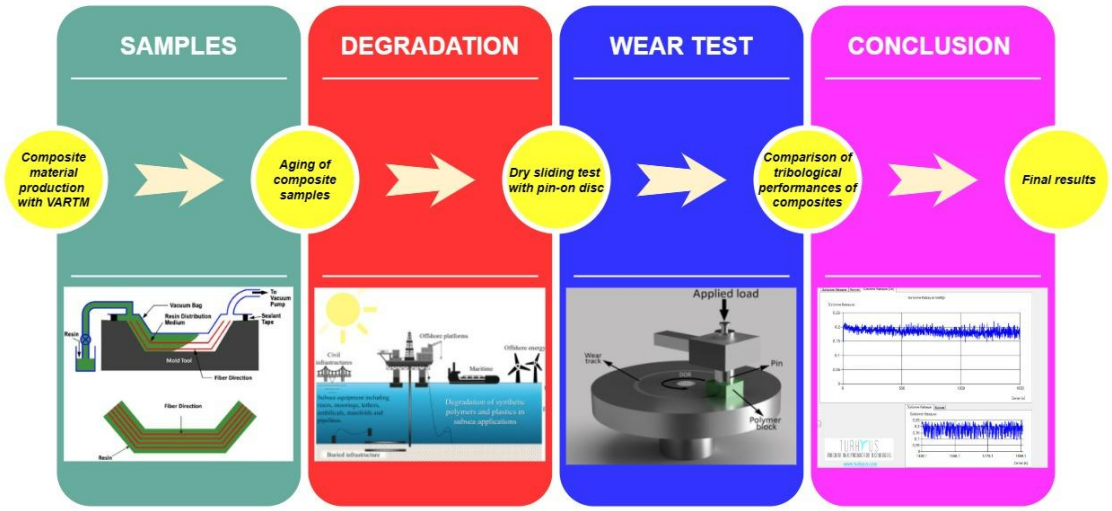

Figure 1. Process scheme of tribological performance of composites.

As the matrix material, a combination of RIMR 135 resin and RIMH 135 hardener epoxy system was used. The mixing ratio of the epoxy system was prepared by weight as 100:30 (RIMR 135 / RIMH 135). The specific properties of the epoxy system are as follows: viscosity (700–1100 mPas), density (1.13–1.17 g/cm³), and flash point (200°C).

Composite plates required for specimen production were manufactured using the vacuum-assisted resin transfer molding (VARTM) technique. Based on preliminary studies, it was determined that for an 8-layer composite plate of dimensions 300 × 330 mm, an epoxy matrix amount corresponding to approximately 65–70% of the fabric weight was sufficient to fully wet the fiber surfaces. During the VARTM process, the appropriate amount of epoxy mixture needed to fully impregnate the reinforcement layers was identified.

The composite samples were produced using the vacuum-assisted resin transfer molding method (VARTM), as illustrated in Figure 2. All composites were kept under vacuum and cured at room temperature (25°C) for 24 hours. The fiber volume fractions of the produced composites were as follows: 50.91% for glass/epoxy composites (GFRP), 56.06% for carbon/epoxy composites (CFRP), and 54.2% for glass-carbon hybrid epoxy composites (GCFRP). The thicknesses of the produced GFRP and CFRP composite plates were 1.90 ± 0.1 mm and 1.85 ± 0.1 mm, respectively. Both GFRP and CFRP composites consisted of eight layers of fiber laminates [29] .

2.2. Aging Processes

Composite specimens reinforced with glass (GFRP) and carbon fibers (CFRP) were fabricated utilizing the Vacuum Assisted Resin Transfer Molding (VARTM) process. Following production, the specimens were machined into appropriate dimensions conforming to the ASTM G99-17 standard, which outlines procedures for wear testing using the pin-on-disc method[30]. After specimen preparation, an aging procedure was conducted under three chemically distinct liquid media, each applied over three separate immersion periods. The characteristic properties of these aging environments are detailed in Table 1, while the distribution of test conditions—including aging duration, fluid medium, and normal load applied during abrasion testing—is presented in Table 2. The composite coupons were immersed in artificial seawater, lubricating oil, and diesel fuel for exposure durations of 30, 60, and 90 days respectively (Figure 3). To simulate a marine-like degradation environment in the laboratory, 35 grams of sodium chloride were precisely weighed and dissolved in tap water until the solution mass reached 1000 grams. The mixture was continuously stirred until complete dissolution was achieved, ensuring homogeneous salinity throughout the solution. For the hydrocarbon-based environments, Shell Helix HX7 10W-40 motor oil was employed to represent a

lubricative industrial exposure condition, while Shell V-Power diesel was used to mimic conditions akin to fuel storage or spillage scenarios. These environments were selected to evaluate the durability and wear response of the composite materials under chemically aggressive and industrially relevant conditions.

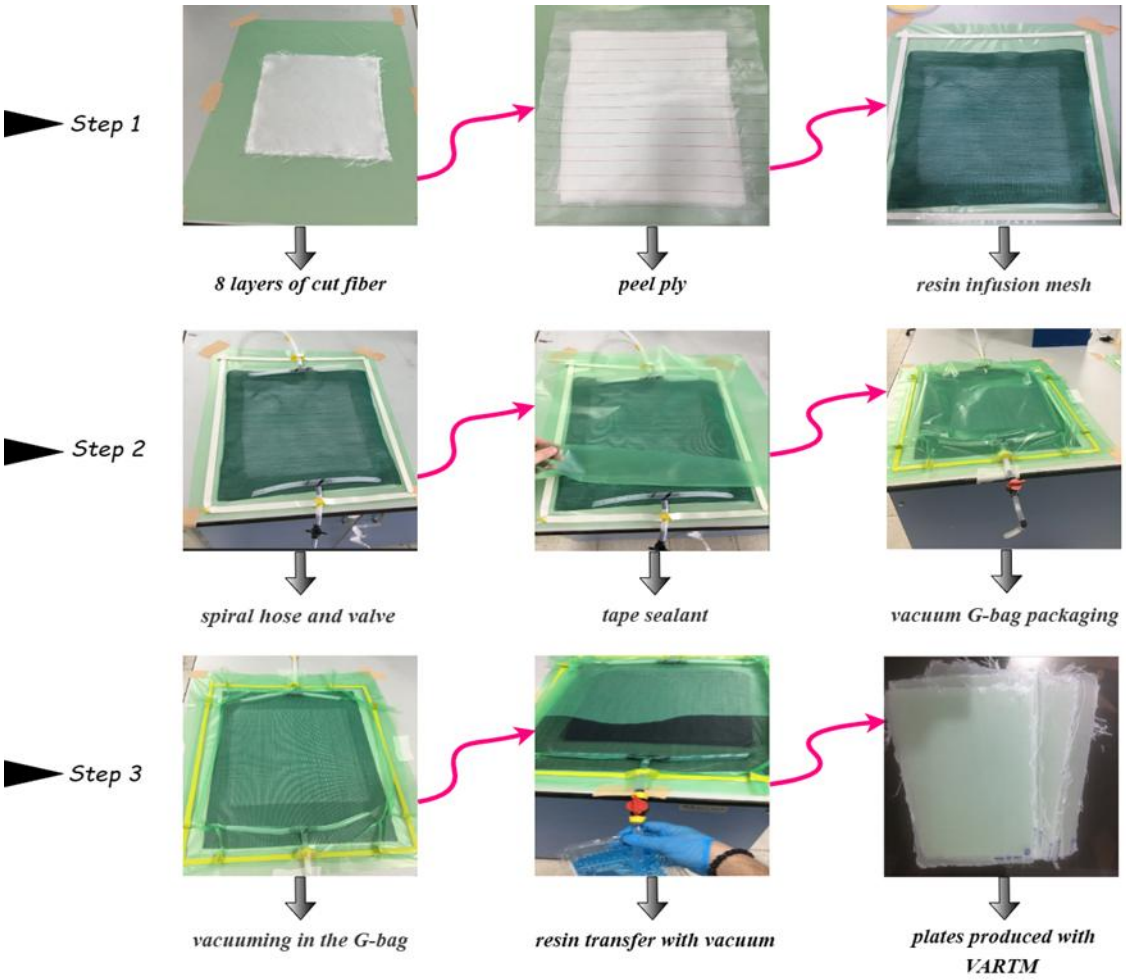

Figure 2. Production of composite plates with VARTM.

This immersion-based preconditioning aimed to simulate potential service environments that the composites might encounter in real-world engineering applications, particularly in the maritime, automotive, and energy sectors.

2.3. Wear Test Using Pin-on-Disk Method

Wear test specimens were prepared from CFRP and GFRP composites produced via VARTM, in accordance with the dry sliding wear test parameters presented in Table 2. A total of 60 specimens were tested under the dry sliding wear conditions defined in Table 2. The specimen geometries used for the wear tests were prepared according to the ASTM G99-17 standard, as illustrated in Figure 4. To obtain the appropriate specimen dimensions for the dry sliding wear tests, the GFRP and CFRP composite plates produced by VARTM were cut using a waterjet cutting machine.

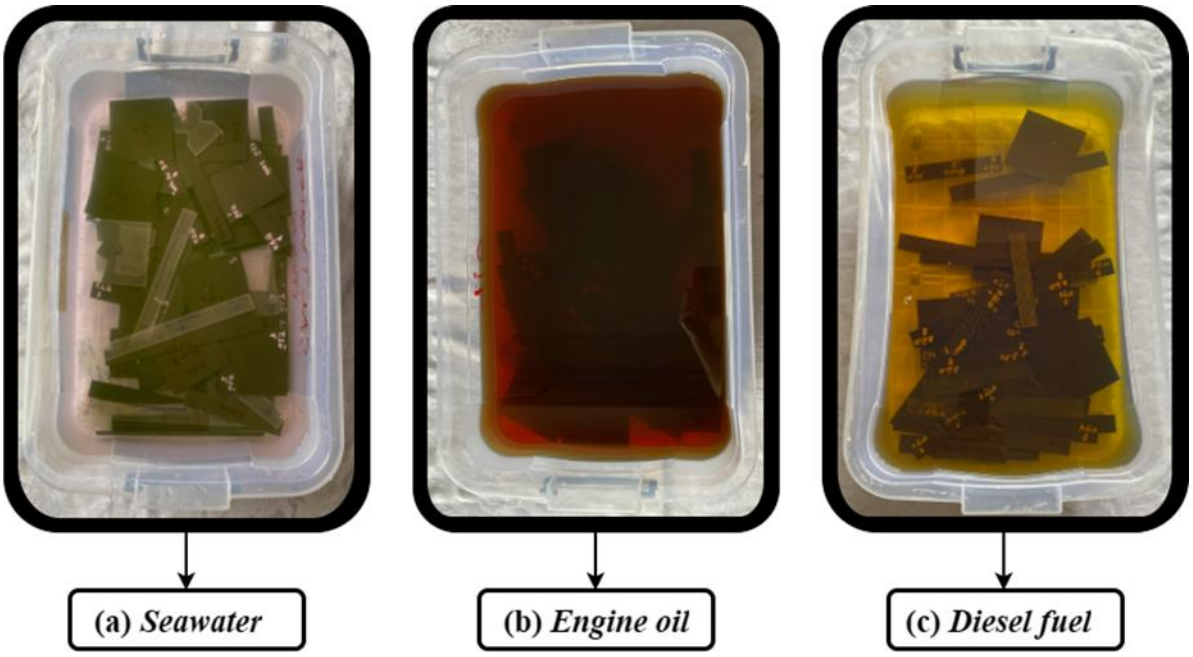

Figure 3. Aging environments of composites: (a) seawater, (b) engine oil, (c) diesel fuel.

Table 1. General physical properties of aging environments [29].

Degradation environment	Density (g/cm3)	Viscosity (MPas)
Seawater	1.023	0.959
Engine oil	0.860	96.310
Diesel fuel	0.832	3.168

Table 2. Test parameters determined for the dry sliding wear test.

Sample	Degradation environment	Aging time (day)			Wear load (Newton)		
GFRP	Room temperature	0	0	0	10	15	20
	Seawater	30	60	90	10	15	20
	Engine oil	30	60	90	10	15	20
	Diesel fuel	30	60	90	10	15	20
CFRP	Room temperature	0	0	0	10	15	20
	Seawater	30	60	90	10	15	20
	Engine oil	30	60	90	10	15	20
	Diesel fuel	30	60	90	10	15	20

Before the tests, the surface roughness of the AISI D2 tool steel disk, used as the counter surface, was measured using a Time TR 3200 surface roughness tester. The measurements were conducted with a sample length of 0.8 mm and an evaluation length of 3 mm to determine the average surface roughness. After completing all wear tests, the surface roughness of the disk was measured again for comparison. The surface roughness measurement process is illustrated in Figure 5. The average surface roughness of the disk before wear was measured as 0.183 μm, and after the wear tests, it increased to 0.753 μm. The mechanical properties of the AISI D2 tool steel disk are presented in Table 3.

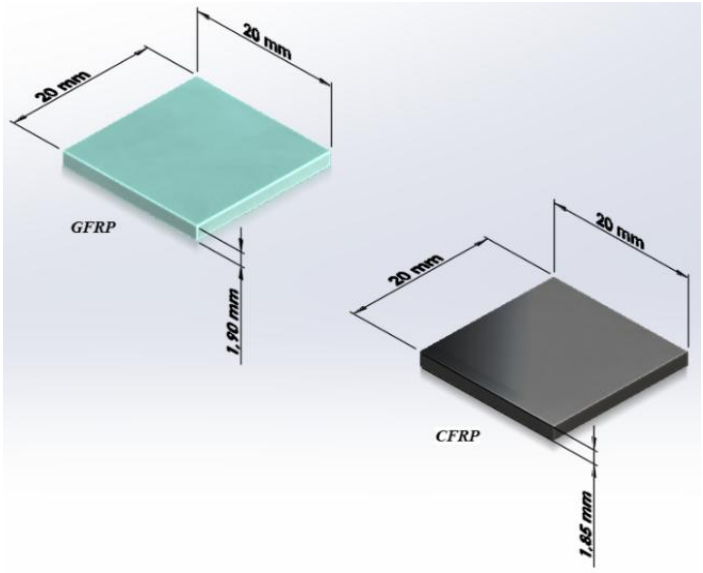

Figure 4. GFRP and CFRP wear test specimen dimensions.

The five-step dry sliding wear test procedure is presented in Figure 6. In the first step, GFRP and CFRP composite specimens, cut into 20×20 mm squares, were prepared. Pins with a diameter of 12 mm were machined from Ø15 mm low-carbon steel rods on a lathe to be mounted on the pin-on-disk wear test machine.

In the second step, the composite specimens were bonded to the 12 mm pins using the Mitre Apel instant adhesive set manufactured by BETA Kimya. Prior to bonding, the pin surfaces were cleaned with acetone to ensure strong and precise adhesion between the composite sample and the pin surface.

In the third step, the weights of the specimens, with and without the pins, were measured using a precision balance before the wear test. These measurements were used to calculate the specific mass wear rate after the tests.

In the fourth step, a counter face disk made of AISI D2 tool steel with dimensions of Ø110×16 mm and a surface hardness of 59 HRC was used. After determining the wear distance based on the selected sliding speed, the test equipment was prepared for operation.

In the fifth step, the wear test machine was activated, and the composite specimens attached to the pins were subjected to dry sliding wear tests against the abrasive disk over the predetermined sliding distance. Tests were conducted under constant sliding distance while varying the applied load. All wear tests were carried out under laboratory conditions at an ambient temperature of 23 °C to assess the tribological behavior of the composite materials.

Figure 5. (a) Wear disk surface, (b) measurement of surface roughness of worn disk surface.

Table 3. Chemical composition and thermal and mechanical properties of AISI D2 tool steel[31].

Properties	Units	Value
Chemical composition		
C	%	1.50
Cr	%	12.00
Mo	%	1.10
Mn	%	0.50
Si	%	0.50
V	%	1.00
Thermal properties		
Thermal conductivity	W/mK	21
Specific heat capacity	J/kg°C	485
Mechanical properties		
Young's modulus	GPa	180
Poisson's ratio		0.3
Density	kg/mm^3	7.64
Hardness	HRC	62±1
Elongation	%	≥16

Figure 6. Pin-on-disc wear testing process steps of GFRP and CFRP composites.

Before starting the dry sliding wear tests, the test parameters were determined and entered into the Turkyus device software on the computer for calculation. First, a sliding speed of 2 m/s was selected as

one of the dry sliding test parameters. Then, a track diameter of 80 mm was chosen, and the device's balance arm was adjusted and calibrated accordingly. The rotational speed (in rpm) required for the abrasive disk to reach a sliding speed of 2 m/s at a track diameter of 80 mm was calculated using Equation (1).

$$n = \frac{6000\, V_c}{d\, \pi} \tag{1}$$

In Equation (1), the variables are defined as follows:
n : Rotational speed (rpm),
Vc : Sliding speed (m/s),
d : Track diameter (mm).

According to this equation, the required rotational speed of the disk was calculated to be n = 477.5 rpm. A reflective tape was attached to the edge of the disk in the Turkyus wear testing device, and the rotational speed was measured using a DT-2236C laser tachometer to determine the inverter frequency corresponding to this speed. As a result, the inverter frequency was identified as 34.3 Hz. Based on preliminary assessments before the wear tests, the sliding distance was set to 3 km. According to the calculated rotational speed, the tests were conducted for 25 minutes to reach this distance. The composite specimen was then mounted on the Turkyus wear test device, and the force arm was balanced horizontally using a spirit level. After entering the calculated values into the Turkyus software, as shown in Figure 7, the wear tests were initiated. The sampling frequency was set to 5 Hz, enabling data collection at five points per second. For each defined test parameter, the sliding speed and dry sliding distance were kept constant, while the applied load was varied as 10 N, 15 N, and 20 N, respectively. During the tests, the coefficient of friction between the wearing composite specimen and the disk surface was recorded and transferred to the computer. The tribological behavior of GFRP and CFRP composites aged in seawater, motor oil, and diesel fuel environments for 30, 60, and 90 days, respectively, was evaluated using this test setup, and the results were interpreted accordingly.

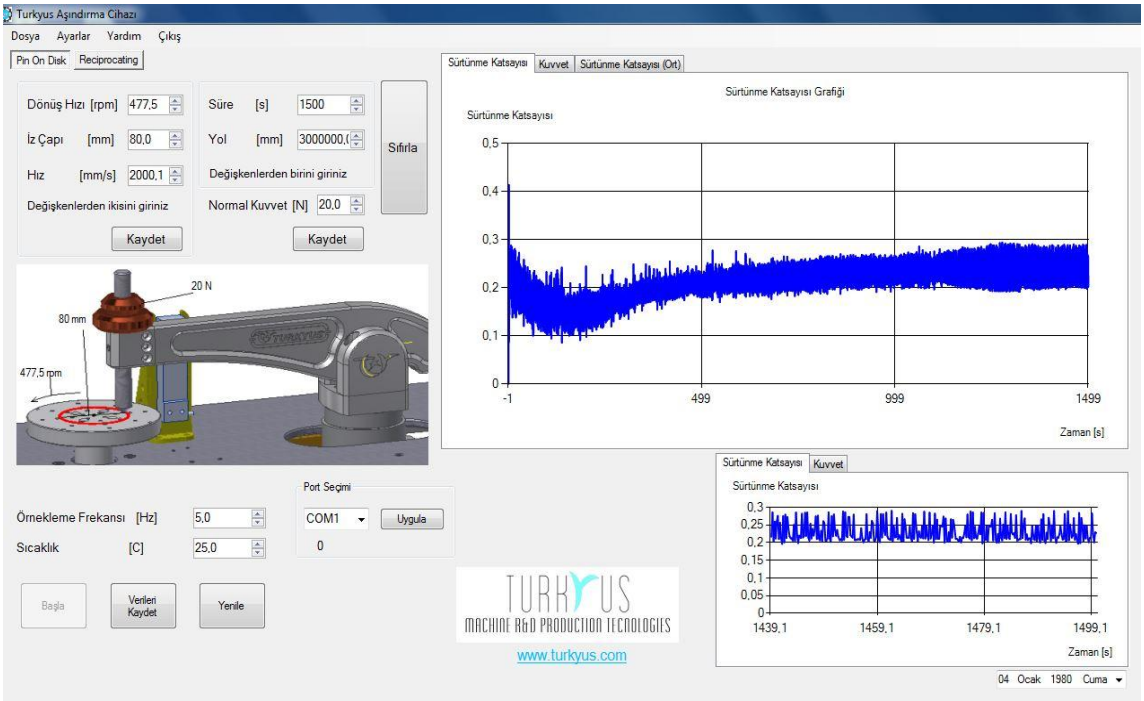

Figure 7. Defining the determined and calculated data for the wear test to the Turkyus wear test device.

According to the eight different parameters listed in Table 2, based on the environmental condition and aging duration of the GFRP and CFRP composites, wear tests were conducted in accordance with the ASTM G99-17 standard. For each parameter, tests were performed at a constant sliding speed of 2 m/s and a fixed sliding distance of 3 km, under three different applied loads (10 N, 15 N, and 20 N). At the beginning and end of each wear test, the composite wear specimens were weighed using a Necklife FA 2004 precision balance with a sensitivity of 0.1 mg. The difference in mass was used to calculate the worn mass. To compare the wear resistance of the composite specimens, the specific wear rate—a reliable parameter—was calculated using Equation (2).

$$W = \frac{\Delta_m}{\rho\, F_N\, S} \tag{2}$$

In Equation (2), the variables are defined as follows:

W : Specific wear rate ($cm^3/N{\cdot}m$),
Δm : Mass Loss (g),
ϱ : Density (g/cm^3),
F_N : Applied load (N),
S : Sliding distance (m).

3. RESULTS

3.1. Coefficient of Friction

Wear tests were conducted on GFRP and CFRP composites aged in seawater, motor oil, and diesel fuel environments for 30, 60, and 90 days, respectively, according to the test parameters presented in Table 2. The wear tests were designed based on parameters such as aging environment, aging duration, and applied load. In each wear test, the sliding speed, sliding distance, and test duration were kept constant, while different loads of 10 N, 15 N, and 20 N were applied. The average coefficient of friction values were calculated for a total of 60 test specimens. The coefficient of friction–load graphs for GFRP and CFRP composites under seawater aging conditions for 30, 60, and 90 days are shown in Figure 8, for the motor oil environment in Figure 9, and for the diesel fuel environment in Figure 10.

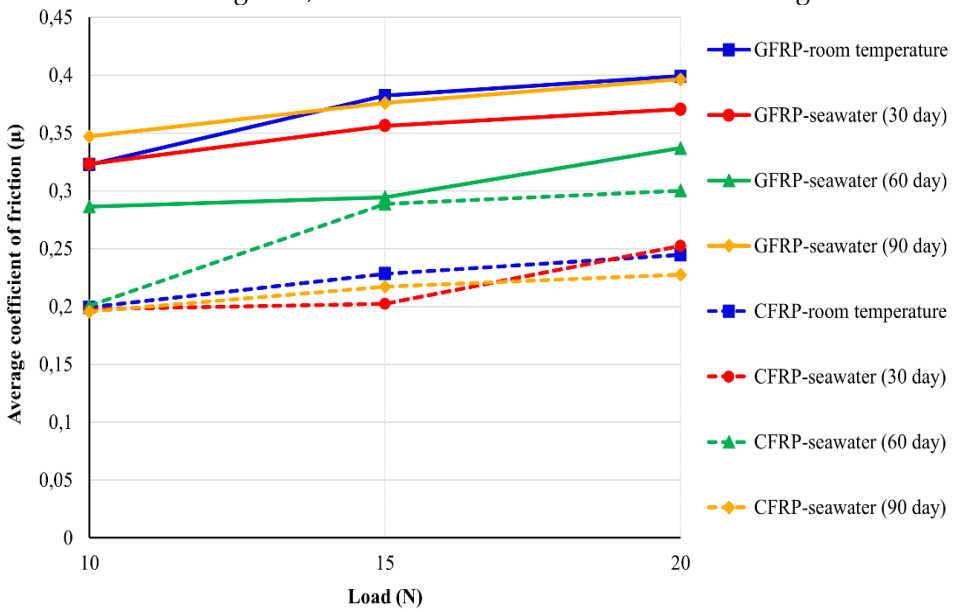

Figure 8. COF-Load graph of GFRP and CFRP composites aged in seawater environment.

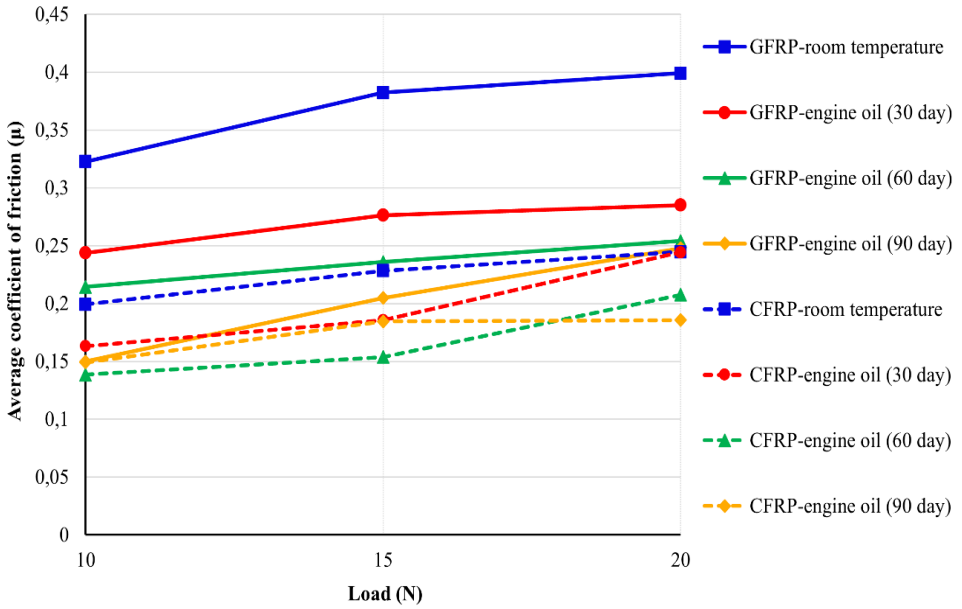

Figure 9. COF-Load graph of GFRP and CFRP composites aged in engine oil environment.

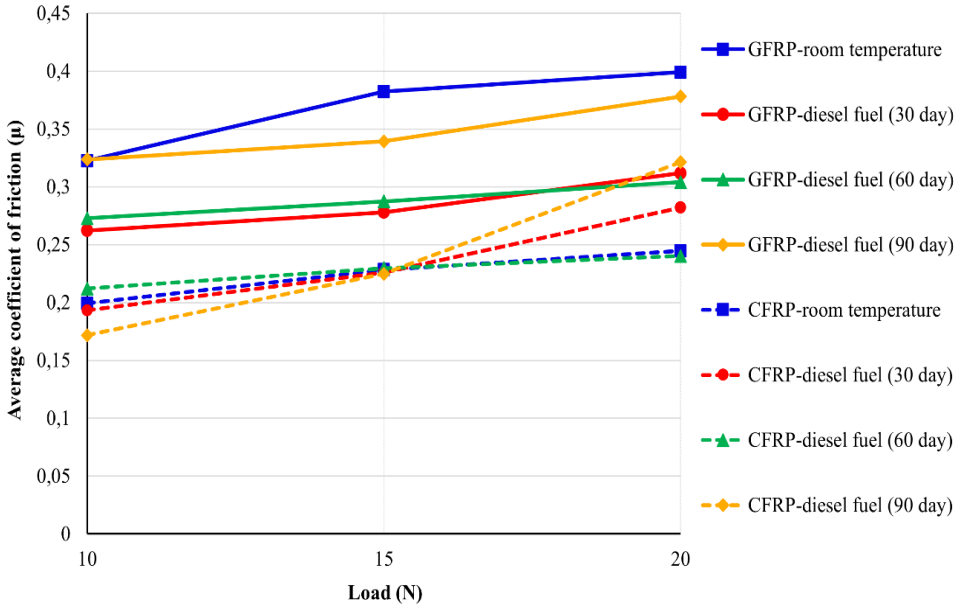

Figure 10. COF-Load graph of GFRP and CFRP composites aged in diesel fuel environment.

As shown in Figure 8, which presents the coefficient of friction (COF) versus load graphs for GFRP and CFRP composites aged in seawater for 30, 60, and 90 days, the following observations were made: Under a 10 N load, the average coefficient of friction for GFRP composites increased by 7.57%, whereas for CFRP composites, it decreased by 1.88% compared to those in the room temperature (unaged) condition after 90 days of seawater aging. Under a 15 N load, the average coefficient of friction decreased by 1.67% for GFRP and by 4.95% for CFRP after 90 days of seawater aging. Under a 20 N load, the coefficient of friction decreased by 0.67% for GFRP and by 6.97% for CFRP under the same aging conditions.

As shown in Figure 9, which illustrates the coefficient of friction (COF) versus load graphs for GFRP and CFRP composites aged in motor oil for 30, 60, and 90 days, the following results were obtained: Under a 10 N load, the average coefficient of friction decreased by 53.52% for GFRP composites and by 25.16% for CFRP composites compared to those in the room temperature (unaged) condition after 90 days of aging in motor oil. Under a 15 N load, the average COF decreased by 46.41% for GFRP and by

19.14% for CFRP after 90 days of exposure to motor oil. Under a 20 N load, the COF decreased by 37.90% for GFRP and by 24.08% for CFRP composites under the same aging conditions.

As shown in Figure 10, which presents the coefficient of friction (COF) versus load graphs for GFRP and CFRP composites aged in diesel fuel for 30, 60, and 90 days, the following results were observed Under a 10 N load, after 90 days of aging in diesel fuel, the average COF increased by 0.35% for GFRP composites, while it decreased by 13.79% for CFRP composites, compared to those in the room temperature (unaged) condition. Under a 15 N load, the COF decreased by 11.25% for GFRP and by 1.57% for CFRP. However, under a 20 N load, the COF decreased by 5.24% for GFRP composites, whereas it increased significantly by 31.39% for CFRP composites after 90 days of exposure to diesel fuel.

3.2. Mass Loss

In the 60 composite test samples of GFRP and CFRP, mass losses occurred due to wear as a result of different aging environments, aging durations, and applied wear loads. To calculate the mass loss between the pre- and post-wear weights, precise measurements were taken using a sensitive balance for each experimental parameter, and the weight losses were calculated accordingly. The mass losses for all aging conditions, material types, and applied loads were computed and are presented in Table 4.

Table 4. Mass losses of GFRP and CFRP composites on pin-on-disc after wear.

Degradation environment	Sample	Applied load (Newton)		
		10 (N)	15 (N)	20 (N)
Room temperature	GFRP	0.0013	0.0022	0.0031
	CFRP	0.0010	0.0015	0.0025
Seawater (30 day)	GFRP	0.0015	0.0024	0.0032
	CFRP	0.0011	0.0017	0.0026
Seawater (60 day)	GFRP	0.0016	0.0027	0.0035
	CFRP	0.0013	0.0019	0.0027
Seawater (90 day)	GFRP	0.0017	0.0030	0.0043
	CFRP	0.0014	0.0023	0.0030
Engine oil (30 day)	GFRP	0.0016	0.0029	0.0038
	CFRP	0.0015	0.0020	0.0032
Engine oil (60 day)	GFRP	0.0018	0.0030	0.0041
	CFRP	0.0019	0.0023	0.0036
Engine oil (90 day)	GFRP	0.0021	0.0034	0.0053
	CFRP	0.0020	0.0029	0.0041
Diesel fuel (30 day)	GFRP	0.0014	0.0023	0.0030
	CFRP	0.0014	0.0021	0.0026
Diesel fuel (60 day)	GFRP	0.0015	0.0025	0.0033
	CFRP	0.0015	0.0023	0.0029
Diesel fuel (90 day)	GFRP	0.0017	0.0027	0.0038
	CFRP	0.0019	0.0025	0.0029

The mass losses observed in the composite specimens in this study are not solely attributed to mechanical wear during dry sliding. Due to the different aging environments and exposure durations, the polymer matrix underwent measurable internal degradation processes such as plasticization, chain scission, and micro void formation. These degradative phenomena significantly alter the density, structural integrity, and adhesion at the fiber-matrix interface, thereby weakening the composite material even before mechanical testing.

In addition, the long-term immersion of specimens in aggressive environments such as seawater, engine oil, and diesel fuel led to significant fluid absorption. This uptake process contributes to changes in specimen mass independent of mechanical wear, and reflects the influence of chemical diffusion, hydrolysis, and swelling within the polymer network. Consequently, the reported mass loss values reflect not only the removal of material due to frictional interaction but also the combined effects of environmental degradation and fluid absorption. This dual mechanism more accurately represents the

tribological behavior of fiber-reinforced polymer composites subjected to coupled mechanical and chemical stress conditions. Recent studies confirm this interpretation. A hygrothermal aging study on multi-filler epoxy composites documented an 11% increase in wear rate and approximately 7% change in mass after accelerated aging cycles [32]. One of the recent studies on moisture absorption in hybrid Kevlar-carbon-glass epoxy composites reported up to 15% increase in water absorption and up to 5-10% increase in wear rate under humid conditions [33]. These findings reinforce the validity of tracking mass change as an integrated metric for evaluating the combined influences of environmental aging and mechanical wear in polymer composite systems.

These findings validate the consideration of total mass loss as a robust metric for evaluating the interplay between environmental aging and dry sliding wear in composite systems. In all environmental conditions, the lowest mass loss for GFRP and CFRP composites was observed in wear tests conducted under 10 N load, while the highest mass loss was observed in tests conducted under 20 N load. Regarding the aging environment conditions, the lowest mass loss occurred in the diesel fuel environment, while the highest mass loss occurred in the motor oil environment. In the motor oil environment, the wear tests conducted under 20 N load showed that the mass loss of the composites after wear increased by 70.96% for glass/epoxy (GFRP) composites and 64% for carbon/epoxy (CFRP) composites compared to the weight loss of the composites in the normal environment. In the seawater environment, wear tests conducted under 20 N load showed that the mass loss of the composites after wear increased by 38.70% for glass/epoxy (GFRP) composites and 20% for carbon/epoxy (CFRP) composites compared to the normal environment. In the diesel fuel environment, wear tests conducted under 20 N load showed that the mass loss of the composites after wear increased by 52% for glass/epoxy (GFRP) composites and 6.45% for carbon/epoxy (CFRP) composites compared to the normal environment.

3.3. Specific Wear Rate (SWR)

One of the reliable parameters used to compare the wear resistance of materials is the specific wear rate. At the beginning and end of the wear test, the samples were weighed using a precision balance, and the difference in mass was calculated to determine the worn mass. The mass losses for 60 samples, presented in Table 4, were used to calculate the specific wear rates using the equation in (2). The wear tests of GFRP and CFRP composites, based on environmental type and aging time, were conducted under the wear rate (2 m/s), sliding distance (3 km), and applied wear load values (10 N, 15 N, and 20 N) in accordance with the ASTM G 99-17 standard. The calculated specific wear rates are presented in Table 5. The specific wear rates of GFRP and CFRP composites for seawater aging environment are shown in Figure 11, for motor oil environment in Figure 12, and for diesel fuel environment in Figure 13.

In Figure 11, the change in the specific wear rate-load graph of GFRP and CFRP composites aged in seawater for 30, 60, and 90 days is shown. It was found that the specific wear rate at 10 N loading increased by 30.769% for GFRP composites and 40% for CFRP composites when aged for 90 days in seawater compared to the ambient temperature condition. At 15 N loading, the specific wear rate increased by 36.36% for GFRP composites and 53.33% for CFRP composites after 90 days of seawater aging compared to the ambient temperature condition. At 20 N loading, the specific wear rate increased by 38.70% for GFRP composites and 20% for CFRP composites after 90 days of seawater aging compared to the ambient temperature condition.

In Figure 12, the change in the specific wear rate-load graph of GFRP and CFRP composites aged in engine oil for 30, 60, and 90 days is presented. It was calculated that the specific wear rate at 10 N loading increased by 61.53% for GFRP composites and 100% for CFRP composites after 90 days of aging in engine oil compared to the ambient temperature condition. At 15 N loading, the specific wear rate increased by 54.54% for GFRP composites and 93.33% for CFRP composites after 90 days of engine oil aging compared to the ambient temperature condition. At 20 N loading, the specific wear rate increased by 70.96% for GFRP composites and 64% for CFRP composites after 90 days of engine oil aging compared to the ambient temperature condition.

Table 5. Specific Wear Rate (SWR) values of GFRP and CFRP composites according to aging environment and applied wear load.

Degradation environment	Sample	Specific wear rate (10-8cm³/Nm)		
		10 (N)	15 (N)	20 (N)
Room temperature	GFRP	2.4208	2.7312	2.8864
	CFRP	2.2371	2.2371	2.7964
Seawater (30 day)	GFRP	2.7932	2.9795	2.9795
	CFRP	2.4608	2.5354	2.9082
Seawater (60 day)	GFRP	2.9795	3.3519	3.2588
	CFRP	2.9082	2.8337	3.0201
Seawater (90 day)	GFRP	3.1657	3.7243	4.0037
	CFRP	3.1319	3.4302	3.3557
Engine oil (30 day)	GFRP	2.9795	3.6002	3.5381
	CFRP	3.3557	2.9828	3.5794
Engine oil (60 day)	GFRP	3.3519	3.7243	3.8175
	CFRP	4.2505	3.4302	4.0268
Engine oil (90 day)	GFRP	3.9106	4.2209	4.9348
	CFRP	4.4742	4.3251	4.5861
Diesel fuel (30 day)	GFRP	2.6070	2.8553	2.7932
	CFRP	3.1319	3.1319	2.9082
Diesel fuel (60 day)	GFRP	2.7932	3.1036	3.0726
	CFRP	3.3557	3.4302	3.2438
Diesel fuel (90 day)	GFRP	3.1657	3.3519	3.5381
	CFRP	4.2505	3.7285	3.2438

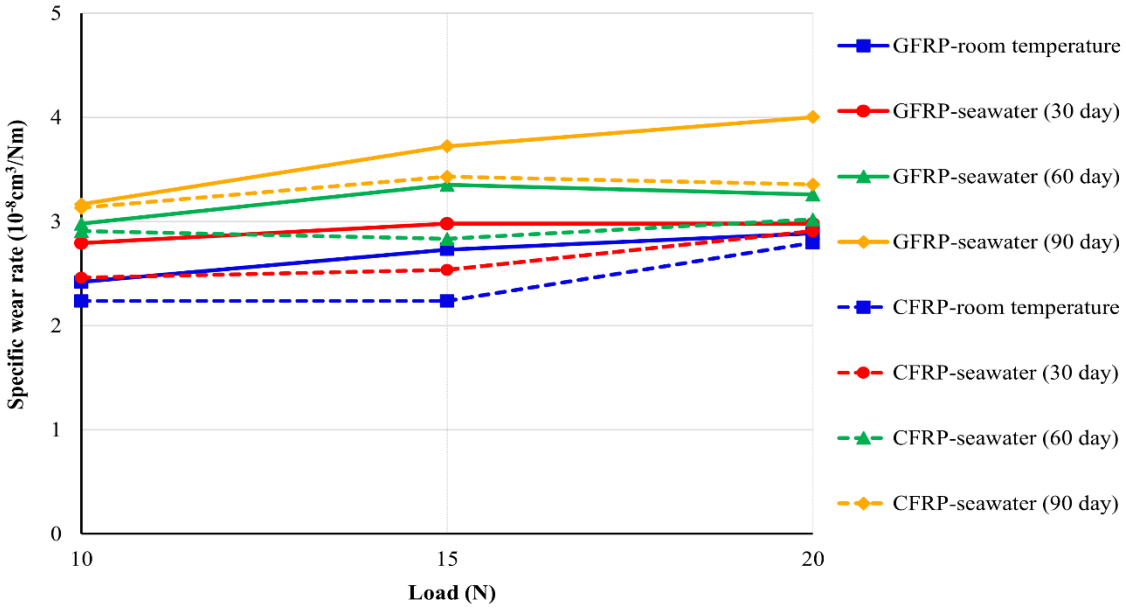

Figure 11. Comparison of Specific Wear Rates of GFRP and CFRP composites aged in seawater.

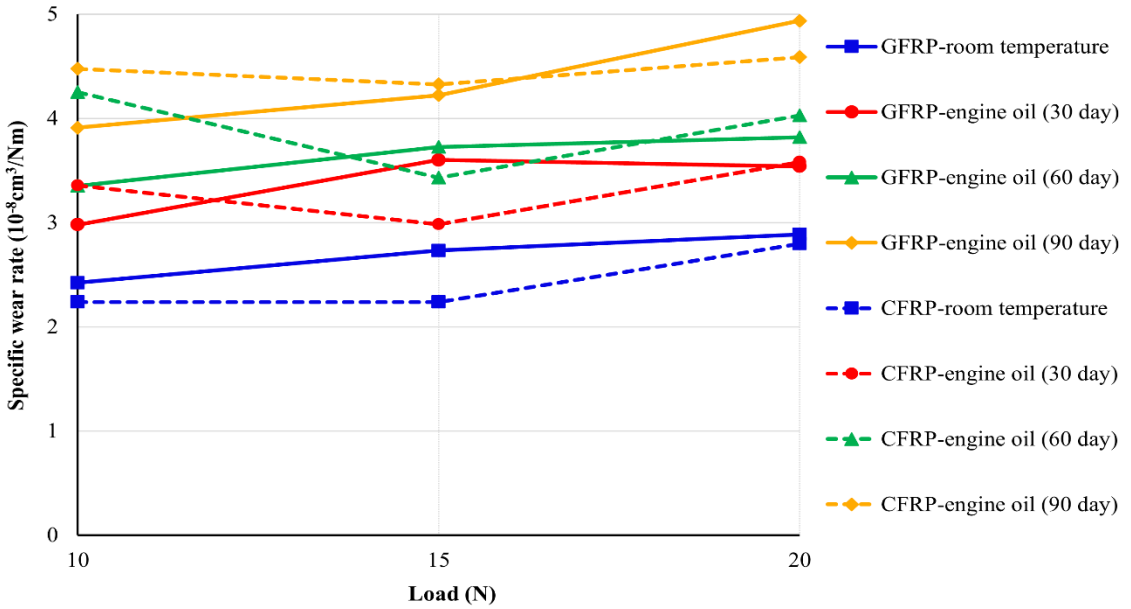

Figure 12. Comparison of Specific Wear Rates of GFRP and CFRP composites aged in engine oil.

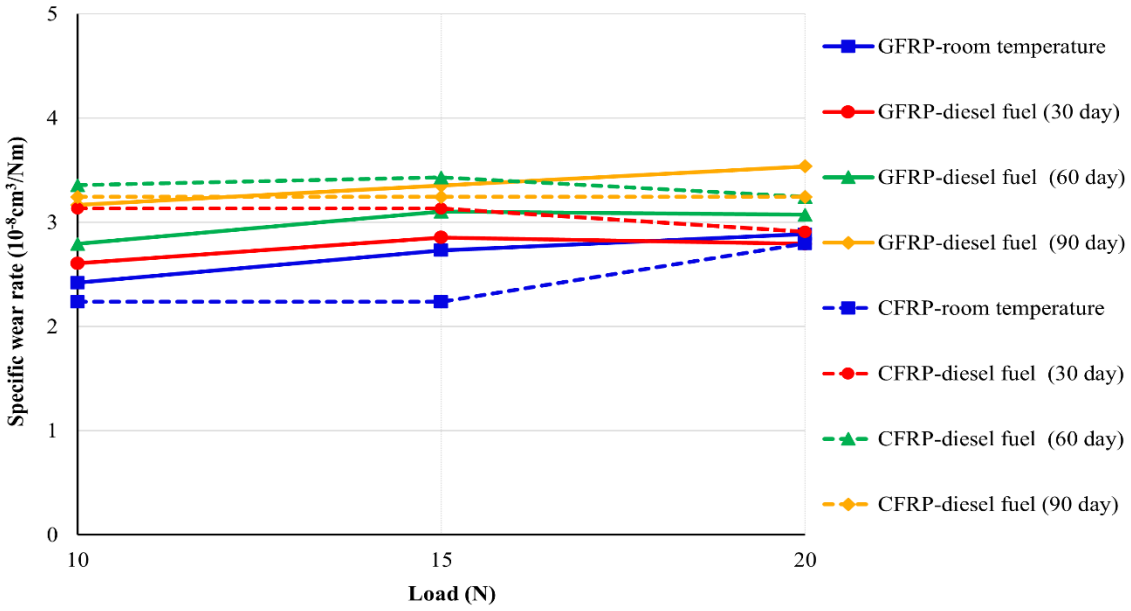

Figure 13. Comparison of Specific Wear Rates of GFRP and CFRP composites aged in diesel fuel.

In Figure 13, the change in the specific wear rate-load graph of GFRP and CFRP composites aged in diesel fuel for 30, 60, and 90 days is shown. It was found that the specific wear rate at 10 N loading increased by 61.53% for GFRP composites and 100% for CFRP composites after 90 days of aging in diesel fuel compared to the ambient temperature condition. At 15 N loading, the specific wear rate increased by 54.54% for GFRP composites and 93.33% for CFRP composites after 90 days of diesel fuel aging compared to the ambient temperature condition. At 20 N loading, the specific wear rate increased by 70.96% for GFRP composites and 64% for CFRP composites after 90 days of diesel fuel aging compared to the ambient temperature condition.

The lowest specific wear rate values for both GFRP and CFRP composites under all environmental conditions were found at 10 N loading, while the highest specific wear rates were observed in the wear tests conducted under 20 N loading.

4. CONCLUSIONS

In this study, the tribological performance of GFRP (Glass Fiber Reinforced Polymer) and CFRP (Carbon Fiber Reinforced Polymer) composites was compared by conducting dry sliding wear tests on a pin-on-disk apparatus after aging in three different environments (seawater, engine oil, and diesel fuel) for 30, 60, and 90 days. The study revealed the sensitivity of the tribological properties of GFRP and CFRP composites to external factors such as applied load, aging environment, and aging duration. The effects of these parameters on the friction coefficient and specific wear rate exhibited an interactive rather than independent relationship. The evaluation was extended across three main axes: load variation, aging environment, and material type.

The effect of load variation generally showed a tendency for the friction coefficient to decrease as the load increased. This phenomenon can be explained by the increased surface area undergoing plastic deformation due to the higher load, and the wear of micro-roughness leading to a smoother surface. In GFRP composites, the change in friction coefficient was more erratic under low load and more affected by the environment, while at high load, environmental effects were less pronounced. This can be attributed to the lower surface hardness of the glass fiber-reinforced structure, which is more susceptible to deformation under load. In CFRP composites, structural stability was achieved under high loads, but the 31.39% increase in the friction coefficient observed under 20 N load in the diesel environment suggests that this load level may cause matrix degradation.

The effect of aging environment played a decisive role in the physical and chemical structure of polymer matrices. The seawater environment, through the diffusion of water into the matrix, can create microscopic voids, disrupting the surface morphology and weakening the fiber-matrix bonds. In GFRP, this effect particularly increased the friction coefficient under low load, while in CFRP, the friction coefficient decreased due to a more limited diffusion effect. The engine oil environment emerged as the most aggressive for GFRP, with the oil penetrating the matrix deeply, causing a plasticizing effect, significantly weakening the fiber-matrix interaction, and reducing friction by creating a lubrication effect on the surface. In CFRP, this effect was less pronounced because of the higher chemical resistance of the carbon fiber structure and the limited matrix diffusion effect. The diesel fuel environment produced relatively more complex results. In GFRP, the increase in the friction coefficient under low load suggested that diesel left chemical residues on the surface, creating a sticky layer, while in CFRP, the significant increase in friction coefficient under 20 N load indicated that diesel fuel could further degrade the carbon fiber-matrix structure.

The effect of aging duration (Time Change): The results from the 30, 60, and 90-day aging periods showed that as the aging time increased, more significant changes occurred in the mechanical and tribological performance of the composites. After 90 days of aging, the environmental effects were observed to reach their maximum level. In particular, the dramatic reduction in the friction coefficient in the engine oil environment for GFRP composites indicated that the oil could penetrate the matrix more over time, potentially leading to permanent surface changes. CFRP composites exhibited more stable behavior over time, indicating that carbon fibers are more resistant to aging effects both chemically and structurally.

The effect of material type: GFRP exhibited a more sensitive behavior towards aging environments due to its more porous structure and weak bonding tendency between glass fiber and the matrix. In contact with liquid environments, physical swelling, fiber separation, and microstructure degradation occurred more quickly, leading to higher variability in tribological performance. CFRP, due to its high strength, low water absorption capacity, and chemical inertness of carbon fibers, showed more stable friction behavior in many environments. However, it was observed that CFRP exhibited less tolerance to structural degradation, particularly under high load in the diesel environment.

The specific wear rate values of GFRP and CFRP composites significantly increased depending on the environment, load, and duration. In all environments, the 90-day aging period caused microstructural degradation in the composites, leading to higher wear rates. In aggressive environments such as engine oil and diesel fuel, significant wear increases were observed in both composites under

10–20 N loads. While CFRP composites were more resistant to friction, they showed higher increases in specific wear rate after aging compared to GFRP, suggesting that the carbon fiber-matrix interface is more sensitive to chemical effects. As the load increased, the wear rate also tended to rise, with a particularly noticeable increase of over 70% in GFRP under 20 N load in the engine oil environment. The results clearly indicate that aging duration and environmental conditions significantly affect the wear performance of GFRP and CFRP composites. After 90 days of exposure under a 20 N load, the specific wear rate of GFRP increased by 70.96% in engine oil, 38.70% in seawater, and 52% in diesel fuel, compared to unaged conditions. For CFRP, these increases were 64%, 20%, and only 6.45% respectively. These findings confirm that engine oil represents the most aggressive environment, while diesel fuel has a relatively milder effect on composite degradation.

These findings highlight the critical importance of environmental selection in the lifespan, friction behavior, and environmental durability of composite materials. When choosing GFRP and CFRP for tribological applications, environmental conditions must be considered, and the material's suitability for lubrication and chemical resistance should be evaluated. Understanding the behavior of fiber-reinforced polymers like GFRP and CFRP under different environmental and load conditions is crucial for determining their suitability for automotive, marine, and industrial applications. In order to develop more durable composite systems for polymers subjected to abrasion under harsh environmental conditions, fiber-matrix interface improvements and long-term durability tests under chemical-thermal-mechanical load combinations are recommended to designers.

Declaration of Ethical Standards

The authors declare that they have no known competing financial interests or personal relationships that could have appeared to influence the work reported in this paper.

Credit Authorship Contribution Statement

Ahmet SAYLIK was responsible for the design and execution of the experiments, data collection, and the writing and editing of the manuscript. Şemsettin TEMİZ contributed primarily to the interpretation and discussion of the results during the manuscript preparation process.

Declaration of Competing Interest

Not Applicable.

Funding / Acknowledgements

The authors gratefully acknowledge that this study was supported by the Scientific Research Projects Coordination Unit of Inonu University (Project ID: FDK-2019-1822).

Data Availability

Not Applicable.

REFERENCES

[1] Y. Wang *et al.*, "A review on energy-efficient manufacturing for high-performance fibre-reinforced composites," *Compos. Part A Appl. Sci. Manuf.*, vol. 192, p. 108779, May 2025, doi: 10.1016/J.COMPOSITESA.2025.108779.

[2] N. E. Ajayi, S. Rusnakova, A. E. Ajayi, R. O. Ogunleye, S. O. Agu, and A. N. Amenaghawon, "A comprehensive review of natural fiber reinforced Polymer composites as emerging materials for sustainable applications," *Appl. Mater. Today*, vol. 43, p. 102666, Apr. 2025, doi:

10.1016/J.APMT.2025.102666.

[3] H. Ünal and A. Kaştan, "Investigation of wear behavior of graphite and wax added polyamide 6," *J. Fac. Eng. Archit. Gazi Univ.*, vol. 37, no. 3, pp. 1237–1245, 2022, doi: 10.17341/gazimmfd.766016.

[4] K. Kumaresan, G. Chandramohan, M. Senthilkumar, B. Suresha, and S. Indran, "Dry Sliding Wear Behaviour of Carbon Fabric-Reinforced Epoxy Composite with and without Silicon Carbide," *Compos. Interfaces*, vol. 18, no. 6, pp. 509–526, 2011, doi: 10.1163/156855411X610241.

[5] A. Talapatra and D. Datta, "A molecular dynamics-based investigation on tribological properties of functionalized graphene reinforced thermoplastic polyurethane nanocomposites," *Proc. Inst. Mech. Eng. Part J J. Eng. Tribol.*, vol. 235, no. 1, pp. 61–78, Jan. 2021, doi: 10.1177/1350650120912612/ASSET/IMAGES/LARGE/10.1177_1350650120912612-FIG10.JPEG.

[6] Z. Tong, J. Du, X. Li, Z. Liu, C. Yan, and W. Lei, "Fabrication and Tribological Properties of Epoxy Nanocomposites Reinforced by MoS2 Nanosheets and Aligned MWCNTs," *Materials (Basel).*, vol. 17, no. 19, p. 4745, Oct. 2024, doi: 10.3390/MA17194745/S1.

[7] U. O. Uyor, A. P. I. Popoola, and O. M. Popoola, "Chemically Functionalized Graphene–Boron Nitride/Polypropylene Nanocomposites with Enhanced Nanomechanical and Anti-wear Properties," *Chem. Africa*, vol. 7, no. 3, pp. 1595–1604, Apr. 2024, doi: 10.1007/S42250-023-00824-Y/FIGURES/8.

[8] N. A, M. Taha, A. M. M. Ibrahim, and A. A. K, "Role of hybrid nanofiller GNPs/Al2O3 on enhancing the mechanical and tribological performance of HDPE composite," *Sci. Reports 2023 131*, vol. 13, no. 1, pp. 1–13, Aug. 2023, doi: 10.1038/s41598-023-39172-9.

[9] M. Ayçiçek, S. Ç. Ayçiçek, N. Özsoy, M. Özsoy, and A. Akinci, "Comparison of Tribological Behaviours of Nano SiO2 and ZrO2 Reinforced Polyester Matrix Composite Materials," *El-Cezeri*, vol. 10, no. 3, pp. 464–474, Sep. 2023, doi: 10.31202/ECJSE.1230975.

[10] İ. Topcu, A. N. Güllüoğlu, M. Kemal Bilici, and H. Ö. Gülsoy, "Investigation of wear behavior of Ti-6Al-4V/CNT composites reinforced with carbon nanotubes," *J. Fac. Eng. Archit. Gazi Univ.*, vol. 34, no. 3, pp. 1441–1449, 2019, doi: 10.17341/gazimmfd.460542.

[11] S. Yalçınkaya, D. Mertgenç, Y. Yolda¸s, and M. Fatih, "Experimental Investigation of the Effect of Seawater on Glass and Carbon Fiber Composites via Mechanical Characterization," *J. Compos. Sci. 2025, Vol. 9, Page 107*, vol. 9, no. 3, p. 107, Feb. 2025, doi: 10.3390/JCS9030107.

[12] W. Lv, T. Wang, Q. Wang, K. K. Yap, F. Song, and C. Wang, "Tribological and Mechanochemical Properties of Nanoparticle-Filled Polytetrafluoroethylene Composites under Different Loads," *Polym. 2024, Vol. 16, Page 894*, vol. 16, no. 7, p. 894, Mar. 2024, doi: 10.3390/POLYM16070894.

[13] Z. Qi, H. Liu, T. He, J. Wang, and F. Yan, "Friction and transfer behavior of alumina nanoparticle-reinforced carbon fiber/polyoxymethylene composites in the deep sea environment," *Tribol. Int.*, vol. 170, p. 107516, Jun. 2022, doi: 10.1016/J.TRIBOINT.2022.107516.

[14] M. Noonan, W. Obande, and D. Ray, "Simulated end-of-life reuse of composites from marine applications using thermal reshaping of seawater-aged, glass fibre-reinforced acrylic materials," *Compos. Part B Eng.*, vol. 270, p. 111118, Feb. 2024, doi: 10.1016/J.COMPOSITESB.2023.111118.

[15] F. Rubino, A. Nisticò, F. Tucci, and P. Carlone, "Marine Application of Fiber Reinforced Composites: A Review," *J. Mar. Sci. Eng. 2020, Vol. 8, Page 26*, vol. 8, no. 1, p. 26, Jan. 2020, doi: 10.3390/JMSE8010026.

[16] D. Stankovic, W. Obande, M. Devine, A. Bajpai, C. M. Ó Brádaigh, and D. Ray, "Accelerated seawater ageing and fatigue performance of glass fibre reinforced thermoplastic composites for marine and tidal energy applications," *Compos. Part C Open Access*, vol. 14, p. 100470, Jul. 2024, doi: 10.1016/J.JCOMC.2024.100470.

[17] P. A. A, P. Sivabalan, V. Mohanavel, and T. Raja, "Investigation of basalt/kevlar fiber-reinforced porcelain filler infused epoxy composite: A viable alternative for marine applications," *Results Eng.*, vol. 25, p. 103928, Mar. 2025, doi: 10.1016/J.RINENG.2025.103928.

[18] Y. Fan, J. Wang, H. Liu, Z. Su, and G. Pei, "The effect of deep-sea pressure during long-term

aging on the tribological performance of fabric-reinforced phenolic composites," *Tribol. Int.*, vol. 202, p. 110344, Feb. 2025, doi: 10.1016/j.triboint.2024.110344.

[19] E. Feyza Sukur, H. Burak Kaybal, H. Ulus, and A. Avci, "Tribological behavior of epoxy nanocomposites under corrosive environment: effect of high-performance boron nitride nanoplatelet," *Sigma J Eng Nat Sci*, vol. 41, no. 2, pp. 385–395, 2023, doi: 10.14744/sigma.2022.00025.

[20] S. Elmas, B. Atac, C. O. Senol, S. Topal, M. Yildiz, and H. S. Sas, "Annealing impact on mechanical performance and failure analysis assisted with acoustic inspection of carbon fiber reinforced poly-ether-ketone-ketone composites under flexural and compressive loads," *Polym. Compos.*, vol. 46, no. 4, pp. 3686–3704, Mar. 2025, doi: 10.1002/PC.29199.

[21] A. Saylık and Ş. Temiz, "Strength and morphological behavior of glass-carbon/epoxy hybrid composite plates aging in seawater, engine oil and diesel fuel degradation environment," *J. Brazilian Soc. Mech. Sci. Eng.*, vol. 46, no. 9, pp. 1–25, Sep. 2024, doi: https://doi.org/10.1007/s40430-024-05119-y.

[22] M. Nikonovich, A. Ramalho, and N. Emami, "Cryogenic cyclic aging effect on thermal, mechanical and tribological performance of PEEK-based materials," *Wear*, vol. 564–565, p. 205709, Mar. 2025, doi: 10.1016/J.WEAR.2024.205709.

[23] M. Nikonovich, A. Ramalho, and N. Emami, "Impact of cryogenic aging and test-environment on mechanical properties and tribological performance of PI-based materials," *Tribol. Int.*, vol. 201, p. 110209, Jan. 2025, doi: 10.1016/J.TRIBOINT.2024.110209.

[24] S. Tamilvanan, A. Tripathy, and A. Ramadoss, "Impact of environmental conditions on the tribological performance of polymeric composites," *Tribol. Polym. Polym. Compos. Polym. Nanocomposites*, pp. 437–466, Jan. 2023, doi: 10.1016/B978-0-323-90748-4.00006-6.

[25] P. H. Sahare, L. P. Dhole, and S. W. Burande, "A review paper on investigation of mechanical and wear properties of polymer composites subjected to environmental degradation," *Mater. Today Proc.*, May 2024, doi: 10.1016/J.MATPR.2024.05.107.

[26] B. Hu *et al.*, "PI/PAI-E44 synthesis-inspired composite coating with graphene-reinforced hydroxyapatite: enhanced wear resistance, antibacterial properties, biological activity, and corrosion resistance," *Surf. Coatings Technol.*, vol. 497, p. 131786, Feb. 2025, doi: 10.1016/J.SURFCOAT.2025.131786.

[27] M. Korku, R. İlhan, and E. Feyzullahoğlu, "Investigation of effects of environmental conditions on wear behaviors of glass fiber reinforced polyester composite materials," *Polym. Compos.*, vol. 46, no. 1, pp. 355–371, Jan. 2025, doi: 10.1002/PC.28992.

[28] A. E. Sahin, E. Yarar, M. O. Bora, and T. Yilmaz, "Investigation of the effect of thermal aging and wear test parameters on the wear behavior of glass fiber (GF) reinforced epoxy composites," *Polym. Compos.*, vol. 45, no. 9, pp. 7820–7832, Jun. 2024, doi: 10.1002/PC.28306.

[29] A. Saylık, "(PDF) Polimer matrisli hibrit kompozitlerin farklı ortam şartlarındaki mekanik ve tribolojik özelliklerinin incelenmesi," Fen Bilimleri Enstitüsü, Malatya, 2022. Accessed: Mar. 12, 2025.[Online].Available:https://tez.yok.gov.tr/UlusalTezMerkezi/TezGoster?key=kIrIdtdJ31bRgjb6fHvMUZWU3LIzP8aWMcIUEFpmgiy8TESRyPvC2J5YkiaVxXbn

[30] "Test Method for Wear Testing with a Pin-on-Disk Apparatus," Jan. 2017, doi: 10.1520/G0099-17.

[31] L. Tang, J. Huang, and L. Xie, "Finite element modeling and simulation in dry hard orthogonal cutting AISI D2 tool steel with CBN cutting tool," *Int. J. Adv. Manuf. Technol.*, vol. 53, no. 9–12, pp. 1167–1181, 2011, doi: 10.1007/s00170-010-2901-2.

[32] J. Tian, X. Qi, and G. Xian, "Effect of hygrothermal aging on the friction behavior and wear mechanism of the multi-filler reinforced epoxy composites for coated steel," *J. Mater. Res. Technol.*, vol. 32, pp. 140–151, Sep. 2024, doi: 10.1016/J.JMRT.2024.07.096.

[33] M. Mani, M. Thiyagu, and P. K. Krishnan, "Effects of moisture absorption analysis of kevlar/carbon/glass/polyurethane epoxy hybrid sandwich composites with nano silicon particles,"*Adv.Mater.Process.Technol.*,Apr.2024,doi:10.1080/2374068X.2024.2342048.